Shaping Inertial Response from Wind Turbines: A Multi-Objective Approach

Faizal Hafiz*, Akshya Kumar Swain*, Nitish Patel* and A. K. Kar†
*Department of Electrical & Computer Engineering, The University of Auckland, Auckland, New Zealand
Email: faizalhafiz@ieee.org, a.swain@auckland.ac.nz
†Department of Electrical Engineering, Unitec Institute of Technology, Auckland, New Zealand
Email: akar@unitec.ac.nz

***Abstract*—The present study proposes an alternate approach to design and shape the Emulated Inertial Response (EIR) from Variable Speed Wind Turbines (VSWT) by exchanging its kinetic energy (KE) with the grid. Although, the KE released by the deceleration of VSWT can momentarily reduce the generation-demand difference, and thereby alleviate the frequency stability, limiting the effects of subsequent VSWT recuperation is one of the major challenge of EIR. The selection of the parameters of inertia controller which can balance the see-saw effects of KE exchange is a difficult task due to non-linear nature of the system . Further, the EIR control parameters must be selected judiciously to satisfy multiple and conflicting power system objectives. To address these issues, the present study uses the notion of Pareto-dominance along with Multi-Objective Particle Swarm Optimization (MOPSO) to select EIR control parameters. The efficacy of the proposed approach has been illustrated via simulations considering a case study on a micro-grid. The simulation results demonstrate that the designed EIR could effectively shape the inertial response as per decision makers requirement.**

***Keywords*—Inertia; load frequency control; multiobjective optimization; particle swarm optimization; variable speed wind turbines**

I. Introduction

A large scale integration of wind resource is a challenging task for the Transmission System Operators (TSO) owing to asynchronous operating nature of Wind Turbines (WT). The lack of ancillary services from WT are major concern for the frequency and the voltage stability. Further, the introduction of significant wind generation in the grid mix usually leads to displacement of conventional generation [1] along with the ancillary services they provide. For this reason, TSO over the world are drawing grid-code requirements for ancillary support services from the WT [2]–[4]. The focus of this article is Emulated Inertial Response (EIR) derived from Variable Speed Wind Turbines (VSWT), a part of solution developed in response to the integration concerns of WT.

The grid inertia is the consequence of the inherent capability of conventional synchronous generators (SG); the synchronous operation enables the exchange of stored Kinetic Energy (KE) in the rotating masses of SG with the grid following the deviations in frequency. This short-term KE exchange with the grid, or inertia, has a pivotal role in damping frequency excursions following generation-demand imbalance, especially during under-frequency events [5]. The inertial response is an ancillary service provided by all Conventional Power Plant (CPP), due to operational characteristics of SG. With the inertia constant (H) in the range of 2-6 s [6], available KE resource in typical modern VSWT is comparable to that of SG in CPP. However, unlike SG, the KE from VSWT is not naturally accessible for the inertial response.

To increase the energy yield, modern VSWT relies on variable rotor speed to track the optimum power point with wind speed variations. The consequent decoupling of the rotor speed from the grid frequency leads to lack of inertial response in VSWT. While the KE resource is present, to utilize it for the purpose of inertial response, it is necessary to somehow link the grid frequency deviations with the active power control of VSWT. Based on this notion, several approaches have been proposed for EIR from VSWT [6]–[13]. Most of the proposed inertia controllers rely either on control signal derived from frequency deviation (Governor, Inertia or Combined Governor-Inertia, referred here as PD) [6], [8], [9], [14] or predefined shaping function (Step Over-Production, referred here as SOP) [10]–[13] to modify power/torque reference. While the possibility of KE release for inertial support is established, the issues related to consequent, and inevitable, KE recovery have received relatively less attention from researchers.

The inertial response derived from VSWT is quite different from SGs inertial response; especially, with regard to KE recovery. Following the KE discharge, the rotor speed of the VSWT must be restored to its optimal value to avoid significant reductions in the energy yield. The ensuing under-production period, in which WT accelerates to track its optimal speed, represents power imbalance which may cause another frequency drop and/or lead to additional burden on the other generators in the grid. The challenge is to exchange KE of VSWT with the grid to reduce frequency nadir while limiting the effects of WT acceleration. To address this issue, a power system objective function containing weighted sum of different objectives have been used to optimize the parameters of inertia controller in [15]–[17]. A weight is assigned to each objective based on the design priority. However, the trail-and-error approach to weights selection is cumbersome and requires multiple runs of the optimization algorithm.

The other concern with the use of EIR is the departure from traditional fish-hook shaped frequency response to the under-frequency events. In this scenario, the desired frequency response may differ based on the requirements of the Decision Maker (DM). For example, when a frequency stability is a major concern, aggressive inertial response may be desired to discharge higher amount of KE from VSWT albeit at

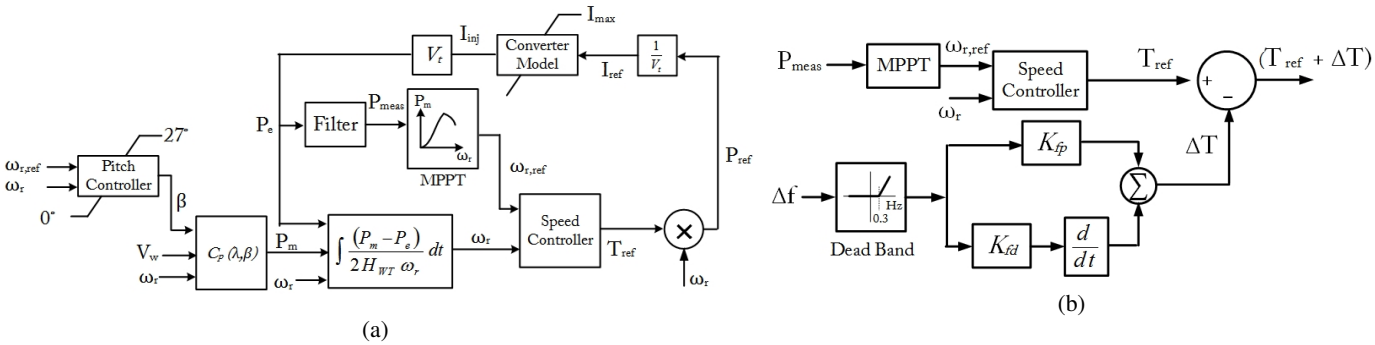

Fig. 1: WT Model and Inertia Controller a) GE 3.6 MW VSWT and b) Governor-Inertia Controller

the expense of increased post-support disturbances due to consequent longer and/or deeper under-production period of VSWT.

It is, therefore, essential to shape/tune the inertial response to obtain the desired frequency response. This is the main focus of this work. A proper selection of control parameters is the key to obtain a desired KE exchange. Since the parameter selection problem consists of multiple and contradictory objectives, a multi-objective power system objective function is proposed to estimate the effects of KE discharge and recovery, i.e., frequency nadir, ROCOF ($\frac{df}{dt}$) and post-support disturbances, respectively. Further, a notion of Pareto-optimality [18] has been used to identify non-inferior parameter pairs that represents varying degree of compromise across design objectives. These parameters pairs can readily be used to shape inertial response as per requirement, e.g., moderate, aggressive. The paper is organized as follows: Section II presents the dynamic power system model used in this work. The proposed approach is detailed in Section III. The simulation results are discussed in Section IV, followed by the conclusion in Section V.

II. System Model

A. Wind Turbine Model

The model of GE 3.6 MW WT is used in this study [19]. The WT employs Doubly Fed Induction Generator (DFIG) and back to back connected PWM converters in the rotor circuit to enable variable speed operation. Based on field-oriented control [20], the power is either extracted from (above rated speed) or injected into (below rated speed) the rotor circuit to control the active power and reactive power injected into the grid. The characteristics of the WT is given by (1).

$$C_p(\lambda,\beta) = \sum_{i=0}^{4}\sum_{j=0}^{4} \alpha_{ij}\,\beta_{ij} \tag{1}$$

The values of α co-efficients in (1) and the other physical parameters are given in Appendix A.

For the simulation purposes, the MPPT behavior of the WT is approximated from the filtered active power, P_{meas}, using (2). More details about the WT model and its controller can be found in Appendix B and [19].

$$\omega_{r,ref} = \begin{cases} 1.2\,pu,\ if\ P_{meas} \geq 0.75\,pu. \\ -.67P_{meas}^2 + 1.42P_{meas} + 0.51,\ otherwise. \end{cases} \tag{2}$$

B. Inertia Controller

A generic Governor-Inertia controller is usually a Proportional and Derivative (PD) controller which is shown in Fig. 1b. Following any disturbance, the derivative control (*Inertia* part) is more effective as the Rate of Change of Frequency (ROCOF, $\frac{df}{dt}$), is higher. Subsequently, the proportional (*Governor* like) control becomes dominant with the increase in Δf.The inertia control is active when the under frequency deviations are larger than $> 300\,mHz$ to avoid the unnecessary stress on the WT. The control action, ΔT is used to update the reference for generator torque, T_{ref}, and hence link the frequency deviations to the active power control loop. Note that, the limits on T_{ref} and active power reference, $P_{WT,ref}$ are unaltered.

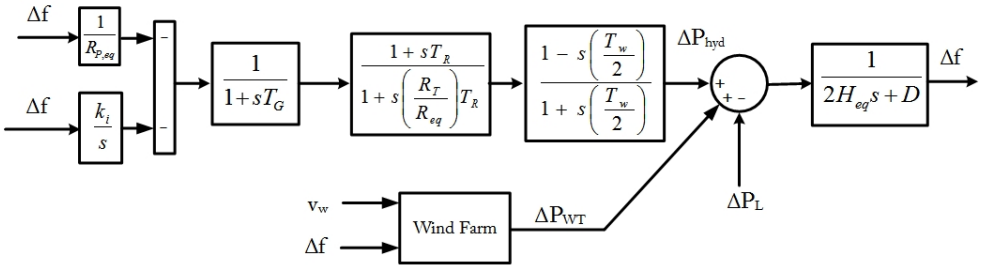

Fig. 2: Test Micro-Grid

C. Test Micro-Grid

The micro-grid containing a Wind Farm and Hydro Power Plant which is investigated in this study is shown in Fig. 2. The wind farm is modelled as a single machine equivalent of 10 GE 3.6 MW WT. The details about the hydro plant are given in Appendix C. In this study, the wind penetration ratio is assumed to be 20% . The generation-demand imbalance is simulated by a step change in load.

III. Proposed Approach

A. Objectives

The main purpose of the inertial response is to exchange the kinetic energy with the grid within short-duration following the disturbance to arrest the fall in grid frequency. Note that, the amount and manner in which the KE is exchanged with the grid have a significant influence on the grid frequency response. This can be achieved by satisfying the following three objectives:

$$min \begin{cases} \theta_1 = (f_{ref} - f_{nadir}) \\ \theta_2 = \max(\frac{df}{dt}) \\ \theta_3 = \sum_{j=0}^{n} (f_{ref} - f)^2, \end{cases} \tag{3}$$

$$subjected\,to: \ \omega_{r,min} < \omega_r < \omega_{r,max},\ P_{WT} \leq P_{WT,max}$$

To prevent the load shedding it is necessary to limit both,the frequency nadir and its rate of change, i.e. Rate Of Change Of Frequency (ROCOF). The first two objective functions, θ_1 and θ_2 (3), are designed to address these concerns. The frequency nadir and ROCOF will be lower with the increasing release of KE. However, a trad-off has to be made during post-support period when WT is regaining the released KE. For example, if the inertial response is too aggressive, i.e. if too much of kinetic energy is extracted from WT, the effects of consequent acceleration/under-production period will be more severe and secondary frequency drop during this period may be equal to or even greater than the original frequency nadir. The third objective function, θ_3, given by (3) takes into account the effects of post-support duration.

Note that, the inertial response is an ancillary service and therefore it is not expected to interfere with the normal operating mode of the VSWT. For this reason it is essential to ensure that WT is operating within its normal operating constraints (e.g. minimum and maximum on limits ω_r and P, limits on ramp rates of P_{ref} and T_{ref}) while providing inertial response. A high penalty is assigned to all the objective functions if any constraint is violated.

B. Multi-Objective Optimization

For multi-objective problems, it is difficult to obtain a single solution which is optimal across all the objectives. Instead, there exist multiple of *non-inferior* or *Pareto Optimal* solutions which are better than the other solutions when all objectives are taken into account, however, not necessarily optimum for each objective [18], [21], [22]. For the parameter selection problem, consider the i^{th} solution (parameter set), $\delta_i = \{k^i_{fp}, k^i_{fd}\}$ and corresponding objective function vector, $\lambda_i = \{\theta_1(\delta_i), \theta_2(\delta_i), \theta_3(\delta_i)\}$. Given two solutions, δ_1 and δ_2, their dominance can be evaluated using their corresponding objective function values based on following condition: $\delta_1\ dominates\ \delta_2$, (denoted as $\delta_1 \preceq \delta_2$)

$$\begin{aligned} &\forall j \in \{1 \dots k\},\ \theta_j(\delta_1) \leq \theta_j(\delta_2) \\ &\wedge\ \exists j \in \{1 \dots k\} : \theta_j(\delta_1) < \theta_j(\delta_2) \\ &\text{with } k = 3\ (no.\ of\ objectives) \end{aligned} \tag{4}$$

The main aim of Multi-Objective (MO) optimization is to find as many non-dominated solutions as possible for the better estimation of the Pareto front, Λ. For this purpose, Multi-Objective Particle Swarm Optimization (MOPSO) [18], is used. Note that, it is possible to use any other multi-objective evolutionary optimization methods like NSGA-II [21], PAES [22] . However, in this study, MOPSO is used for its implementation advantages.

The conventional PSO (*designed for single objective optimization*) relies on a cognitive memory and social interactions of mass less particles for the search of a promising region in the fitness landscape. In each iteration, each particle's next movement is evaluated based on it's previous best record and that of a single learning exemplar. To handle multiple objectives, MOPSO uses *non-dominated sorting* for fitness ranking along with an additional external archive to store non-dominated (Pareto optimal) solutions. Unlike, conventional PSO, multiple learning exemplars from the external archive (*representing non-dominated solutions*) are used as a learning exemplar. For each particle, a different learning exemplar is selected from the external archive through roulette-wheel selection. The external archive is updated in each iteration to store the non-dominated/Pareto optimal solutions i.e. a single run of MOPSO can provide multiple Pareto optimal solutions. More details about the algorithm can be found in [18].

C. Parameter Selection

The set of Pareto optimal solutions obtained after optimization represents non-inferior solutions with varying degree of compromise across design objectives. Usually, the selection of final solution from the Pareto optimal solutions is left to engineering judgment of the decision maker. However, to make the selection process simpler and more intuitive, the following procedure is adopted in this work.

Consider a Pareto optimal set, Δ (5), and a Pareto Front, Λ (6), containing *n* Pareto optimal solutions which are obtained after the Multi-Objective Optimization. The aim is to design a simple measure to rank compromise represented by each Pareto solution. For this purpose, each objective (θ) is normalized in the range of [0,1] using its minimum and maximum value across *n* Pareto solutions, as shown in (7). After normalization, the degree of compromise of the i^{th} solution (δ_i) is estimated by evaluating the 1-Norm (9) of its corresponding objective function vector ($\overline{\lambda}_i$) (8). The solution with minimum Norm-1, $\|\overline{\lambda}\|_1$, represents minimum compromise across all objectives.

$$\Delta = [\delta_1, \delta_2 ... \delta_n] \tag{5}$$

$$\Lambda = [\lambda_1, \lambda_2 ... \lambda_n] \tag{6}$$

TABLE I: SELECTED PARAMETERS FROM THE PARETO FRONT

	Paramater Set (δ)		$\|\overline{\lambda}_i\|_1$	Remarks
PD-1	0.97	1.00	1.00	$minimum\ \theta_1\ and\ \theta_2$
PD-2	0.43	1.00	0.53	$minimum\ \|\overline{\lambda}_i\|_1$
PD-3	0.15	0.28	0.97	$mid-range$
PD-4	0.28	0.87	0.57	$from\ knee-point\ region$

TABLE II: COMPARATIVE EVALUATION OF SELECTED PARETO SOLUTIONS

	No-Support	PD-1	PD-2	PD-3	PD-4
$\Delta\omega_{r,max}\ (pu)$	-	0.54	0.21	0.08	0.15
$\Delta P_{WT,max}\ (pu)$	-	0.44	0.29	0.13	0.23
$t_{inj}\ (s)$	-	15.08	12.48	10.75	11.33
$f_{min}\ (Hz)$	48.31	49.01	48.90	48.57	48.83
$\dot{f}\ (Hz/s)$	0.9016	0.9014	0.9014	0.9016	0.9017
$Post-Support\ f_{min}$	-	49.32	49.37	49.39	49.36

$$\overline{\theta}_k(\delta_i) = \frac{\theta_k(\delta_i) - \theta_{k,min}}{\theta_{k,max} - \theta_{k,min}}, \quad \textit{where } k = \{1,2,3\},\ \textit{no. of objectives} \tag{7}$$

with $\theta_{k,min} = \min_{\delta_1,\ldots\delta_n} \theta_k(\delta_i)$ and $\theta_{k,max} = \max_{\delta_1,\ldots\delta_n} \theta_k(\delta_i)$

$$\overline{\lambda}_i = [\overline{\theta}_1(\delta_i),\ \overline{\theta}_2(\delta_i),\ \overline{\theta}_3(\delta_i)] \tag{8}$$

$$\|\overline{\lambda}_i\|_1 = \sum_{j=1}^{3} |\overline{\theta}_j(\delta_i)| \tag{9}$$

Since, the PD inertia controller has only two parameters (k_{fp}, k_{fd}), it is possible to visualize different Pareto solutions and corresponding $\|\overline{\lambda}\|_1$, as shown in Fig. 3b. Note that, for this problem there exists a knee-point (region with lower $\|\overline{\lambda}\|_1$). From Fig. 3b, it is observed that in the knee point region, the value of k_{fp} and k_{fd} lies in the range of [0.3,0.5] and [0.88,1], respectively. On the basis of these observations, four Pareto solutions were selected (as shown in Table I), to highlight differences in compromise represented by different Pareto solutions. The first parameter set, 'PD-1', is selected as it corresponds to the minimum of the first two objectives. The second set, 'PD-2', represents overall best compromise with minimum $\|\overline{\lambda}\|_1$. The other two sets, 'PD-3' and 'PD-4', are selected from different regions of the Pareto front.

Note that the kinetic energy available for the inertial support is a non-monotonic function of WT operating point (wind speed, v_w) and its operational limitations [15]. For this reason any selected parameter set will maintain the expected pefromance in a very narrow range around the design operating point ($8.5\,m/s$ in this study). To maintain a desired inertial response throughout the operating range of WT, the parameter selection process can be repeated for several operating points which can further be used to derive an adaptive inertia controller. The detailed studies on these topics can be found in our preivous works [15], [17].

IV. RESULTS

To evaluate the efficacy of selected parameter sets, generation-demand imbalance was simulated in the test microgrid (Fig. 2), by $0.1\,pu$ step change in load demand, ΔP_L. The consequent responses of WT, Hydro Turbine and grid

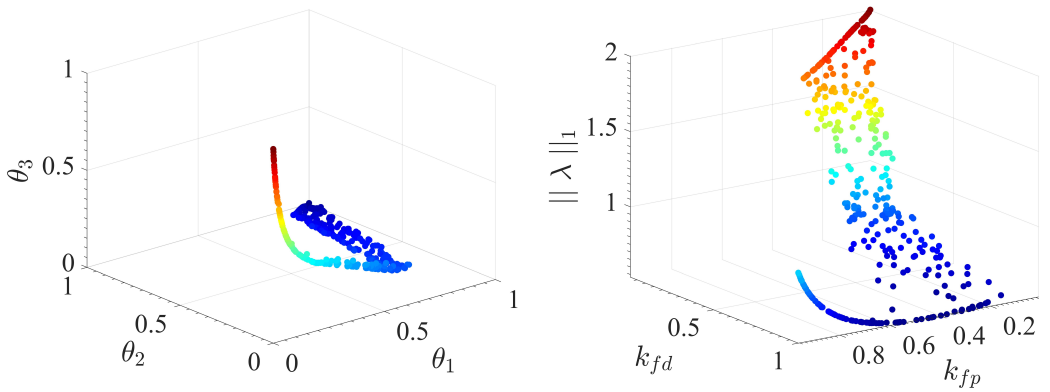

Fig. 3: (a) Pareto Front obtained after Optimization and (b) Pareto Solutions and Corresponding $\|\overline{\lambda}\|_1$

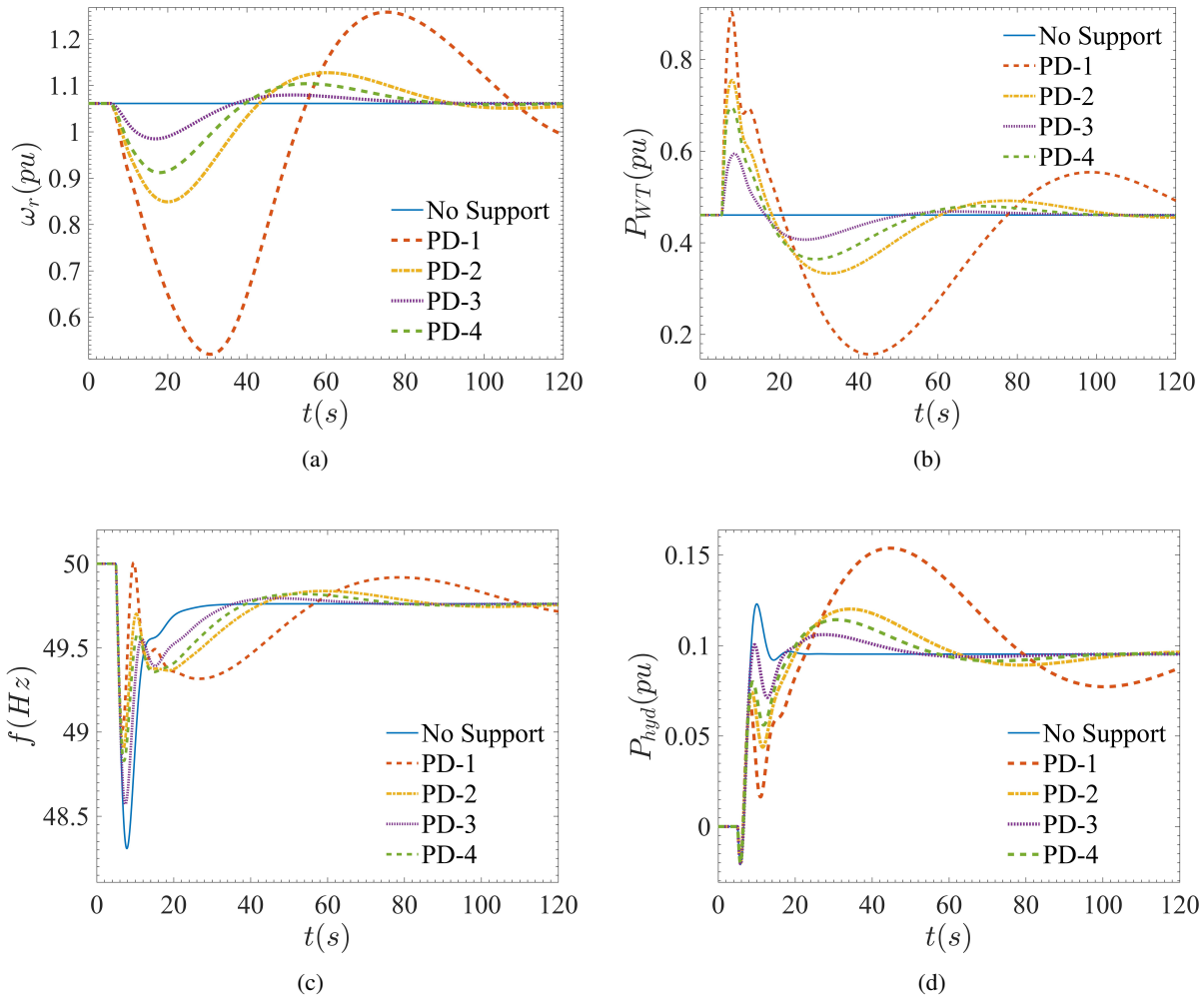

Fig. 4: Response of WT and Hydro-Plant with different parameter settings following the disturbance (0.1 pu at 5 s): a) Active Power Injected by WT b) Deviation in WT rotor speed c) Grid frequency response and d) Active Power Response of the hydro power plant

frequency are shown in Fig. 4. The performance metrics used to evaluate inertial response are listed in Table II.

As expected, the inertial response obtained with PD-1 is very aggressive. Hence, KE released to the grid is maximum (among compared parameter sets) and it is reflected in the plot of $\Delta\omega_r$ shown in Fig. 4a. The higher KE release leads to the active power injection, ΔP_{WT}, (shown in Fig. 4b) having the highest magnitude and the longest duration, t_{inj}, among compared parameter sets. As a result, maximum improvement in frequency nadir, f_{min} (shown in Fig. 4c) and ROCOF (Table II) is obtained . Note that, for the emulated inertial response, kinetic energy exchange with the grid is slightly negative, i.e., slightly more KE is required to restore the WT to its pre-disturbance operating point. The higher amount of KE release, due to aggressive tuning, will result in longer and/or deeper KE recovery and, hence, a compromise is made in post-support disturbances. This can be observed in the results obtained with PD-1, for which the secondary frequency drop, $Post - Support\, f_{min}$, is highest (Table II) and the stress on Hydro Turbine, ΔP_{hyd}, is even more than *no-support* scenario (Fig. 4d). On the other hand, PD-3, favors limited post-support effects by trading off limited release of kinetic energy. However, due to limited KE release and consequent lower active power injection, the improvement in frequency and ROCOF is lowest as shown in fig. 4 and Table II.

With the other two parameter sets, PD-2 and PD-4, the kinetic energy exchange is more balanced and hence better trade-off is achieved across all the objectives. Especially, with PD-2, which represents the Pareto solution with minimum $\|\overline{\lambda}\|_1$, reduction in frequency nadir is achieved with limited post-support disturbance (Table II).

V. Conclusion

The inertial response design problem is approached as Multi-Objective optimization problem to yield several non-inferior or Pareto optimal parameter settings. With the proposed framework, multiple of Pareto optimal settings can be obtained representing varying degree of compromise across

design objectives. Any of the obtained Pareto optimal parameter settings can be used based on a design preference. For example, in a weaker grid, where frequency stability is a major concern, Parameter setting corresponding to aggressive inertial response, e.g. PD-1, can be used. On the other hand, when post-support disturbance are of concern, parameter settings leading to limited kinetic energy release, e.g. PD-3, may be preferred.

In addition, a simple method to facilitate the ranking of Pareto optimal solution based on Norm-1 potential of normalized objective function vector, $\|\overline{\lambda}\|_1$, is proposed. It was shown that, the Pareto optimal solution with minimum $\|\overline{\lambda}\|_1$ represents the best overall compromise across all the design objectives among all the Pareto optimal solutions. For this reason, in the absence of any design preference, inertial parameter settings corresponding to minimum $\|\overline{\lambda}\|_1$ are recommended.

APPENDIX A
WT PHYSICAL PARAMETERS

R=52 m, H_{WT}=5.19 s, $0.5\rho A_r$=0.00145, λ_{opt}=8.25, $C_{p,opt}$=0.5023

C_p Co-efficients: $\alpha_{0,0}$ = -4.1909e-01, $\alpha_{0,1}$ = 2.1808e-01, $\alpha_{0,2}$ = -1.2406e-02, $\alpha_{0,3}$ = -1.3365e-04, $\alpha_{0,4}$ = 1.1524e-05, $\alpha_{1,0}$ = -6.7606e-02, $\alpha_{1,1}$ = 6.0405e-02, $\alpha_{1,2}$ = -1.3934e-02, $\alpha_{1,3}$ = 1.0683e-03, $\alpha_{1,4}$ = -2.3895e-05, $\alpha_{2,0}$ = 1.5727e-02, $\alpha_{2,1}$ = -1.0996e-02, $\alpha_{2,2}$ = 2.1495e-03, $\alpha_{2,3}$ = -1.4855e-04, $\alpha_{2,4}$ = 2.7937e-06, $\alpha_{3,0}$ = -8.6018e-04, $\alpha_{3,1}$ = 5.7051e-04, $\alpha_{3,2}$ = -1.0479e-04, $\alpha_{3,3}$ = 5.9924e-06, $\alpha_{3,4}$ = -8.9194e-08, $\alpha_{4,0}$ = 1.4787e-05, $\alpha_{4,1}$ = -9.4839e-06, $\alpha_{4,2}$ = 1.6167e-06, $\alpha_{4,3}$ = -7.1535e-08, $\alpha_{4,4}$ = 4.9868e-10

APPENDIX B
WT CONTROLLERS

Pitch Controller: $(k_{pp} + \frac{k_{ip}}{s})$, with k_{pp}=150, k_{ip}=25
Speed Controller: $(k_{pw} + \frac{k_{iw}}{s})$, with k_{pw}=3.0, k_{iw}=0.6
Converter Model: $(\frac{1}{1+sT_{con}})$, with T_{con}=0.02 s
Filter: $(\frac{1}{1+sT_f})$, with T_f=5.0 s

APPENDIX C
HYDRO PLANT PARAMETERS

T_G=0.2 s, T_W=1.0 s, T_R=5.0 s, $R_{p,eq}$=0.05, R_T=0.38, H_{eq}=3.0 s, D=1.0 s

REFERENCES

[1] D. Lew and R. Piwko, "Western wind and solar integration study," *National Renewable Energy Laboratories, Technical Report No. NREL/SR-550-47781*, 2010.

[2] M. Tsili and S. Papathanassiou, "A review of grid code technical requirements for wind farms," *Renewable power generation, IET*, vol. 3, no. 3, pp. 308–332, 2009.

[3] *The network code on load-frequency control and reserves*, ENTSO-E, Brussels, 2013.

[4] *The grid code. 2012. Issue 4, Revision 13.*, National Grid Company plc, UK, 2012.

[5] P. Kundur, N. J. Balu, and M. G. Lauby, *Power system stability and control*. McGraw-hill New York, 1994, vol. 7.

[6] J. Morren, S. W. H. de Haan, W. L. Kling, and J. A. Ferreira, "Wind turbines emulating inertia and supporting primary frequency control," *IEEE Transactions on Power Systems*, vol. 21, no. 1, pp. 433–434, Feb 2006.

[7] N. W. Miller, R. W. Delmerico, K. Kuruvilla, and M. Shao, "Frequency responsive controls for wind plants in grids with wind high penetration," in *2012 IEEE Power and Energy Society General Meeting*, July 2012, pp. 1–7.

[8] J. Morren, J. Pierik, and S. W. de Haan, "Inertial response of variable speed wind turbines," *Electric Power Systems Research*, vol. 76, no. 11, pp. 980 – 987, 2006.

[9] G. Ramtharan, J. B. Ekanayake, and N. Jenkins, "Frequency support from doubly fed induction generator wind turbines," *IET Renewable Power Generation*, vol. 1, no. 1, pp. 3–9, March 2007.

[10] N. R. Ullah, T. Thiringer, and D. Karlsson, "Temporary primary frequency control support by variable speed wind turbines-potential and applications," *IEEE Transactions on Power Systems*, vol. 23, no. 2, pp. 601–612, May 2008.

[11] P. K. Keung, P. Li, H. Banakar, and B. T. Ooi, "Kinetic energy of wind-turbine generators for system frequency support," *IEEE Transactions on Power Systems*, vol. 24, no. 1, pp. 279–287, Feb 2009.

[12] G. C. Tarnowski, P. C. Kjar, P. E. Sorensen, and J. Ostergaard, "Variable speed wind turbines capability for temporary over-production," in *2009 IEEE Power Energy Society General Meeting*, July 2009, pp. 1–7.

[13] A. D. Hansen, M. Altin, I. D. Margaris, F. Iov, and G. C. Tarnowski, "Analysis of the short-term overproduction capability of variable speed wind turbines," *Renewable Energy*, vol. 68, pp. 326 – 336, 2014.

[14] N. Miller, D. Manz, H. Johal, S. Achilles, L. Roose, and J. P. Griffin, "Integrating high levels of wind in island systems: Lessons form hawaii," in *Intelligent System Application to Power Systems (ISAP), 2011 16th International Conference on*, Sept 2011, pp. 1–8.

[15] F. Hafiz and A. Abdennour, "Optimal use of kinetic energy for the inertial support from variable speed wind turbines," *Renewable Energy*, vol. 80, pp. 629–643, 2015.

[16] F. M. Hafiz and A. Abdennour, "Optimal inertial support from the variable speed wind turbines using particle swarm optimization," *IFAC-PapersOnLine*, vol. 48, no. 30, pp. 78–83, 2015.

[17] F. Hafiz and A. Abdennour, "An adaptive neuro-fuzzy inertia controller for variable-speed wind turbines," *Renewable Energy*, vol. 92, pp. 136–146, 2016.

[18] C. A. C. Coello, G. T. Pulido, and M. S. Lechuga, "Handling multiple objectives with particle swarm optimization," *IEEE Transactions on Evolutionary Computation*, vol. 8, no. 3, pp. 256–279, June 2004.

[19] K. Clark, N. W. Miller, and J. J. Sanchez-Gasca, "Modeling of ge wind turbine-generators for grid studies," *GE Energy*, vol. 4, 2010.

[20] L. Xu and P. Cartwright, "Direct active and reactive power control of dfig for wind energy generation," *Energy Conversion, IEEE Transactions on*, vol. 21, no. 3, pp. 750–758, 2006.

[21] K. Deb, A. Pratap, S. Agarwal, and T. Meyarivan, "A fast and elitist multiobjective genetic algorithm: Nsga-ii," *IEEE Transactions on Evolutionary Computation*, vol. 6, no. 2, pp. 182–197, Apr 2002.

[22] J. D. Knowles and D. W. Corne, "Approximating the nondominated front using the pareto archived evolution strategy," *Evolutionary computation*, vol. 8, no. 2, pp. 149–172, 2000.